

Monolayers of Symmetric Triblock Copolymers at the Air–Water Interface. 2. Adsorption Kinetics

Mercedes G. Muñoz,[†] Francisco Monroy,^{*,‡} Francisco Ortega,[†]
Ramón G. Rubio,[†] and Dominique Langevin[‡]

Departamento de Química Física I, Facultad de Ciencias Químicas, Universidad Complutense, E28040 Madrid Spain, and Laboratoire de Physique des Solides, LPS CNRS, Bâtiment 510, Université Paris-Sud, F91405 Orsay, France

Received February 10, 1999. In Final Form: July 22, 1999

Dynamic surface tension (DST) experiments have been combined with time-resolved ellipsometry (TRE) to study the adsorption kinetics of symmetric triblock copolymers at the air–water interface. The equilibrium behavior of these adsorbed monolayers has been studied in the preceding paper in this issue (part 1), pointing out evidence for brush formation at sufficiently high surface concentrations. The dynamic results are consistent with a diffusive mechanism delayed by adsorption barriers in the full adsorption regime at lower concentrations. The first-order phase transition scenario evidenced from the equilibrium results is now also perceptible from the dynamic results: a competition between the bulk diffusion and molecular reorientation mechanisms is found in the brush regime. This two-step adsorption kinetics is characterized by an intermediate plateau, $d\gamma(t)/dt = 0$, which gives evidence for phase coexistence while final steady-state equilibrium is attained.

1. Introduction

In a preceding paper in this issue,¹ we have described studies of the equilibrium properties of adsorbed and spread films of water-soluble poly(ethylene oxide) (PEO)–poly(propylene oxide) (PPO) symmetric triblock copolymers, (PEO–PPO–PEO). 2D first-order phase transitions, characterized by constant surface pressure branches in the isotherm, *i.e.*, $(d\Pi/d\Gamma)_T = 0$, have been observed. These phase transitions, unusual in water-soluble surfactants, are caused by the grafting ability of the studied triblock polymers at the air–water interface, which lead to the formation of a brush phase. The brush was made of folded polymer chains anchored at the interface by the more hydrophobic central PPO block and with the lateral PEO blocks dangling in the adjacent aqueous subphase.¹ The study of the adsorption kinetics of these polymeric surfactants at the air–water interface was intended to complete the equilibrium results, and to clarify the mechanisms for brush formation and the first-order nature of the observed phase transitions. In this context, dynamic surface tension (DST) and time-resolved ellipsometric (TRE) measurements were carried out to follow the adsorption kinetics, and they have allowed us to measure the adsorbed amount $\Gamma(t)$ from the bulk as a function of time.

An outline of this paper is as follows: Section 2 is devoted to a brief theoretical background on adsorption kinetics. The experimental details concerning the dynamical experiments are given in section 3. More details about the systems can be found in the experimental section in the first paper (see section 3 in ref 1). The experimental results are presented in section 4 and are discussed in section 5. Finally, section 6 summarizes the main conclusions.

* To whom correspondence should be addressed. E-mail: monroy@eucmos.sim.ucm.es.

[†] Universidad Complutense.

[‡] Université Paris-Sud.

(1) Muñoz, M. G.; Monroy, F.; Ortega, F.; Rubio, R. G.; Langevin, D. *Langmuir* **1999**, *13*, xxxx.

2. Theoretical Framework

2.a. Mass Transfer in the Bulk. The first step of the adsorption of surface active molecules at a freshly formed air–water interface involves the diffusion-mediated material transport from the bulk. If a *Fickian*-like diffusion is assumed in the z -direction (perpendicular to the surface plane), the dynamic equation for material transport from the bulk can be written as

$$\partial c(z,t)/\partial t = D\nabla^2 c(z,t) \quad (1)$$

with the following limit and boundary conditions:

$$c = c_s \quad \text{at} \quad t \rightarrow \infty \quad \text{and} \quad z = 0 \quad (2)$$

$$\frac{\partial \Gamma(t)}{\partial t} = J_{\text{diff}}(t) = -D \left(\frac{\partial c}{\partial z} \right)_{z=0} \quad (3)$$

c_s being the bulk concentration in the subsurface, *i.e.*, at $z = 0$, and D the diffusion coefficient of the surfactant in the bulk. Equation 3 stands for mass conservation at the interface.

The solution of these equations is the well-known Ward and Tordai equation, which has an integral form:²

$$\Gamma(t) = 2c \left(\frac{Dt}{\pi} \right)^{1/2} - 2 \left(\frac{D}{\pi} \right)^{1/2} \int_0^{t^{1/2}} c_s(t-\tau) d\tau^{1/2} \quad (4)$$

At short times and sufficiently low concentration the surface molecules interact quasi-ideally. In this case, the following approximated expression can be given for dynamic surface tension:^{2,3}

$$\gamma(t) \approx \gamma_0 - 4RTc(D_{\text{short}}t/\pi)^{1/2} \quad \text{at} \quad t \rightarrow 0 \quad (5)$$

On the other hand, if the bulk-to-surface transport is always diffusion-controlled, a $\gamma(t) \sim t^{-1/2}$ dependence is found at long times:³

(2) Ward, A. F.; Tordai, L. *J. Chem. Phys.* **1946**, *14*, 453.

(3) Fainerman, V. D.; Makievski, A. V.; Miller, R. *Colloids Surf.*, **1994**, *87*, 61.

$$\gamma(t) \approx \gamma_{\text{eq}} + \frac{R\Gamma^2}{c} \left(\frac{\pi}{D_{\text{long}}t} \right)^{1/2} \quad \text{at } t \rightarrow \infty \quad (6)$$

In these approximated equations γ_0 and γ_{eq} are the solvent surface tension and the equilibrium values, respectively. If pure Fickian diffusion is the only mechanism for mass transport to the interface, one should find $D_{\text{short}} = D_{\text{long}} = D$. However, apparent values of the diffusion coefficient could be obtained from eqs 5 and 6 if additional mass transport mechanisms coexist within pure diffusion.

2.a. Adsorption–Desorption Kinetics. Once the surfactant reaches the bulk region adjacent to the surface, also called the *subsurface*, the transfer to the surface is frequently assumed to obey a first-order rate kinetics; *i.e.*, Langmuir adsorption is assumed:

$$d\Gamma(c;t)/dt = J_{\text{diff}}(c) + J_{\text{ads}}(c) - J_{\text{des}}(c) \quad (7)$$

where the adsorption and desorption fluxes can be written as

$$J_{\text{ads}}(c) - J_{\text{des}}(c) = k_A c_s (\Gamma_{\infty} - \Gamma) - k_D \Gamma \quad (8)$$

In this mass balance equation k_A and k_D are the adsorption and desorption kinetic constants, respectively, which account for the activation energy of both processes:

$$k_A = k_A^{(0)} \exp(-E_A/RT) \quad \text{and} \quad k_D = k_D^{(0)} \exp(-E_D/RT) \quad (9)$$

Although these kinetic equations (eqs 7–9) cannot be solved analytically, the Ward and Tordai short-time solution given in eq 5 is always valid since adsorption–desorption effects are much slower than the diffusion-mediated initial stage.^{4,5} However, at long times, deviations from the pure diffusive dependence given in eq 6 arise either from the influence of the adsorption–desorption process,^{4,5} or from slower processes such as molecular reorientation at the surface after adsorption.⁶

In practice, if adsorption kinetics is not diffusion-controlled and an adsorption barrier exists, D_{eff} values lower than the real values D are found when using eq 6.⁷ Liggieri et al. have demonstrated that this diffusion-adsorption mixed mechanism corresponds to a renormalized diffusion kinetics where the adsorption barrier E_A is accounted for by an effective diffusion coefficient:^{4,5}

$$D_{\text{eff}} \equiv D_{\text{long}} = D \exp(-E_{\text{act}}/RT) \quad (10)$$

with $E_{\text{act}} = E_A - E_D$ the activation energy for the Langmuir-like adsorption process in eqs 8 and 9.

Their calculations showed that relatively small barriers can have a significant effect on $\Gamma(t)$ at long times. For example, for a saturated monolayer at equilibrium, at $t = 10$ s, the predicted adsorption Γ for $E_{\text{act}} = 1.1RT$ and $3.2RT$ is 5 and 10 times lower than that for the purely diffusion-controlled model, respectively.⁵ Recently, the analysis of $\gamma(t)$ data of nonionic^{8–11} and ionic¹¹ surfactant

solutions has led to the conclusion that there is a crossover from a diffusion-controlled mechanism at dilute concentrations to a mixed diffusion–kinetic-controlled one at more elevated bulk concentration. The case of diffusion-controlled adsorption followed by molecular reorientation at the interface has been theoretically handled by Joos et al.,⁶ leading to

$$\gamma(t) \approx \gamma_{\text{eq}} + [(\gamma_0 - \gamma_{\text{eq}} - B) \exp(-4t\pi\tau_D)^{1/2} + B] \exp(-t/\tau_R) \quad (11)$$

where B and τ_R are, respectively, the amplitude and characteristic time of the reorientation process, and τ_D is the diffusion relaxation time given by

$$\tau_D = \frac{1}{D} \left(\frac{d\Gamma}{dc} \right)^2 \quad (12)$$

When $B=0$ and $\tau_R^{-1}=0$, the purely diffusive approximate solution found earlier by Joos and Serrien is recovered:¹²

$$\gamma(t) \approx \gamma_{\text{eq}} + (\gamma_0 - \gamma_{\text{eq}}) \exp(-4t\pi\tau_D)^{1/2} \quad (13)$$

2.c. Equilibrium Adsorption Isotherm. At equilibrium, the rate of change of $\Gamma(t)$ in eq 7 vanishes, and the adsorption equation or Γ – c equilibrium relationship can be obtained:

$$\Theta = \frac{\Gamma}{\Gamma_{\infty}} = \frac{c}{c+a} \quad (14)$$

where the Szyszkowsky concentration a or concentration at $\Theta = 1/2$ is given by

$$a = \frac{k_D^{(0)}}{k_A^{(0)}} \exp\left(\frac{E_A - E_D}{RT}\right) \quad (15)$$

It is worth noting that this adsorption equation, also called *generalized Frumkin*, is only valid for surfactants which form a 2D monolayer (full adsorption regime). In the brush regime, relevant to the polymers studied here, new interactions of the nonadsorbed 3D material in the brush cause an additional decrease of γ with respect to the full adsorbed state at $\Gamma = \Gamma_{\infty}$. If the activation energies in eq 9 for the adsorption and desorption processes are assumed to be independent of surface coverage, the *Langmuir* equation of state is obtained:

$$\gamma_{\text{eq}}(\Gamma) = \gamma_0 + RT\Gamma_{\infty} \ln(1 - \Gamma/\Gamma_{\infty}) \quad (16)$$

3. Experimental Section

3.a. Chemicals. Two different symmetrical (PEO)_A–(PPO)_B–(PEO)_A triblock copolymers (Pluronic) of different molecular weights and relative chain lengths (A/B) have been used in this study. Both polymers, hereinafter *Pluronic I* (Synperionic F68 from Fluka, Germany) and *Pluronic II* (from PolySciences, Germany), were used as received without further purification. These polymers are the same as those studied in the earlier paper concerning the equilibrium properties of both adsorbed and spread monolayers.¹ Further details on their chemical structure and characterization and the experimental procedure for the preparation of the monolayers are given in ref 1.

3.b. Dynamic Techniques. To measure the long-time (> 1 s) adsorption kinetics of the considered triblock copolymers at the air–water interface, we have combined dynamic surface tension (DST) and time-resolved ellipsometry (TRE) measurements. A

(4) Ravera, F.; Liggieri, L.; Steinchen, A. *J. Colloid. Interface Sci.* **1993**, *156*, 109.

(5) Liggieri, L.; Ravera, F.; Passerone, A. *Colloids Surf.*, **A1996**, *114*, 351.

(6) Serrien, G.; Geeraerts, G.; Ghosh, L.; Joos, P. *Colloids Surf.* **A1992**, *68*, 219.

(7) Defay, R.; Petré, G. *Surface and Colloid Science*; Matjevic, E., Ed.; Wiley: New York, 1979.

(8) Lin, S. Y.; Tsai, R. Y.; Lin, L. W.; Chen, S. I. *Langmuir* **1996**, *12*, 6530.

(9) Colin, A.; Giermanska-Kahn, J.; Langevin, D.; Desbat, B. *Langmuir* **1997**, *13*, 2953.

(10) Chang, H. C.; Hsu, C. T.; Lin, S. Y. *Langmuir* **1998**, *14*, 2476.

(11) Li, B.; Geeraerts, G.; Joos, P. *Colloids Surf.*, **A1994**, *88*, 251.

(12) Serrien, G.; Joos, P. *J. Colloid Interface Sci.* **1990**, *139*, 149.

detailed description of both experimental techniques and their operative principle has been done elsewhere.¹

Concerning DST, successive readings of the instantaneous surface tension $\gamma(t)$ were made at constant intervals of 1 s after a fresh surface is formed by aspiration of the air–solution interface with a *Pasteur* pipet connected to a vacuum pump. Obviously, there is a lack of precision in the determination of the end point of the aspiration process, which corresponds to the starting point of the $\gamma(t)$ curve. However, the time needed to reach γ_{eq} in the considered systems goes from a few minutes for the more concentrated samples to more than 1 day for the more diluted samples; consequently an inaccuracy of 1–2 s in the effective age of the interface is not a problem here. On the other hand, due to the long duration of the experiments, care was taken to minimize evaporation of the solvent.

To obtain the adsorbed amount Γ as a function of time, the instantaneous values of the ellipsometric angle $\Delta(t)$ were registered every six s until equilibrium was established. The refraction index of the film n and the film thickness d cannot be independently calculated from the variations of the ellipsometric angle Δ . However, its product nd is an invariant quantity, independent of the layer model considered.¹³ Hence, the total amount of adsorbed polymer $\Gamma(t)$ is proportional to the variation of the ellipsometric angle $\Delta(t)$ through¹⁴

$$\Gamma(t) = dc_s = d(n - n_1)/(\partial n_1/\partial c) \propto \delta\Delta(t) \quad (17)$$

where c_s is the polymer concentration in the layer and $(\partial n_1/\partial c)$ the change in refractive index of the aqueous solution with polymer concentration. This method has been successfully applied to follow the adsorption kinetics at solid–liquid interfaces.¹⁴

4. Experimental Results

For the sake of clarity of the subsequent analysis some equilibrium results and conclusions derived from the equilibrium data in the previous paper¹ must be recalled here. Briefly, from the combined analysis of the equilibrium isotherms and ellipsometric data of the adsorbed and spread monolayers of two different Pluronic samples, the appearance of a brush phase in equilibrium with a fully adsorbed phase was evidenced at $c = c_1$. A complete polymer brush is obtained at $c \geq c_2$. The coexistence region is characterized by constant pressure sections in the isotherms. The first-order character of the transition is also supported by simultaneous observations of the film textures by means of Brewster angle microscopy.¹ To analyze the mechanisms for polymer adsorption at the air–water interface, and to clarify the first-order phase transition scenario sketched in the previous paper, we have combined time-resolved surface tension (DST) and ellipsometric (TRE) measurements. Figure 1 shows the $\gamma(t)$ curves for Pluronic I at different polymer bulk concentrations. For the sake of clarity, only some of the $\gamma(t)$ curves obtained in the high dilution regime ($c \leq 6 \times 10^{-5}$ mM) have been represented in Figure 1a, while curves obtained at larger concentrations ($c \geq 6 \times 10^{-5}$ mM) have been represented in Figure 1b. It can be observed that, for $c \leq 6 \times 10^{-5}$ mM, $\gamma(t)$ extrapolates to the solvent value γ_0 at $t \rightarrow 0$, whereas an apparent initial value lower than the solvent value, $\gamma(t \rightarrow 0) < \gamma_0$, is clearly observed at higher c . This seems to point out the bimodal character of the adsorption kinetics in this concentration range. It is important to remark that the change observed in the adsorption kinetics takes place at the concentration $c \approx c_2$, where a complete brush is formed.¹ A characteristic time of the slower rate-limiting step of the adsorption kinetics can be obtained by fitting the $\gamma(t)$ curves to an

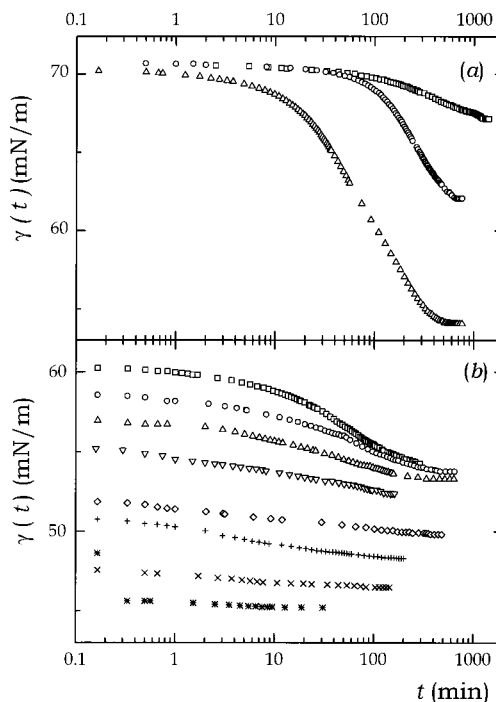


Figure 1. (a) Experimental $\gamma(t)$ curves from DST experiments, obtained at $T = 20 \pm 1$ °C for the adsorbed monolayers of Pluronic I. Bulk concentrations c expressed in mM: (a) (\square) 1.7×10^{-6} ; (\circ) 2.39×10^{-6} ; (\triangle) 7.17×10^{-6} ; (b) (\square) 4.84×10^{-5} ; (\circ) 6.71×10^{-5} ; (\triangle) 1.59×10^{-4} ; (∇) 3.64×10^{-4} ; (\diamond) 1.37×10^{-3} ; (+) 2.13×10^{-3} ; (\times) 3.57×10^{-3} ; (*) 5.78×10^{-3} .

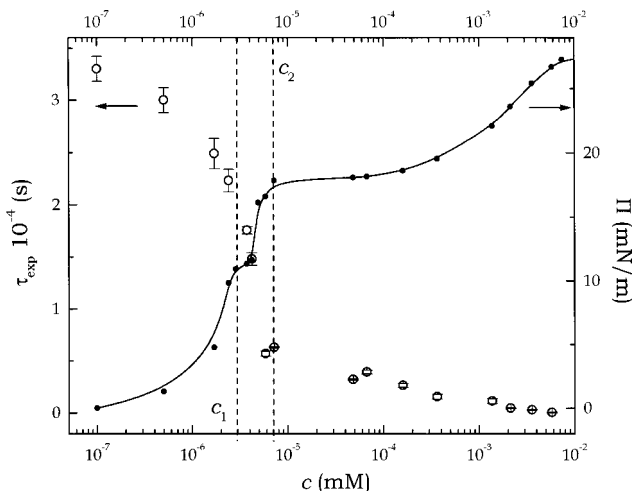


Figure 2. Effective time for surface formation τ_{eff} as a function of bulk concentration for adsorbed monolayers of Pluronic I at $T = 20 \pm 1$ °C. For comparison with the different surface regimes, the equilibrium Π – c isotherm is also shown: $c \leq c_1$, full adsorption regime; $c \geq c_2$, brush regime; $c_1 < c < c_2$, coexistence regime.

exponential dependence, $\gamma(t) = \gamma_0 - \Delta\gamma \exp(-t/\tau_{\text{eff}})$. Figure 2 shows the results for the effective surface formation time τ_{eff} . For the sake of comparison, the equilibrium Π – c data have also been incorporated. A strong decrease of τ_{eff} for Pluronic I is clearly observed at $c \approx c_2 \approx 10^{-5}$ mM, when the second Π plateau starts at ~ 19 mN/m. The variation of τ_{eff} is also remarkably similar to that of the ellipsometric thickness $\delta\Delta$ (see Figure 1b in ref 1).

For comparison purposes, three of the experimental $\Delta(t)$ curves obtained from the data from TRE experiments for Pluronic I in the brush regime are shown in Figure 3. While there is a strong increase of the adsorbed amount $\Gamma(t) \approx \delta\Delta(t)$, the time for total equilibration increases only

(13) Azzam, R. M. A.; Basara, N. M. *Ellipsometry and Polarized Light*; North-Holland: Amsterdam, 1992.

(14) Dorgan, J. R.; Stamm, M.; Toprakcioglu, C.; Jérôme, R.; Fetters, L. J. *Macromolecules* **1993**, *26*, 5321.

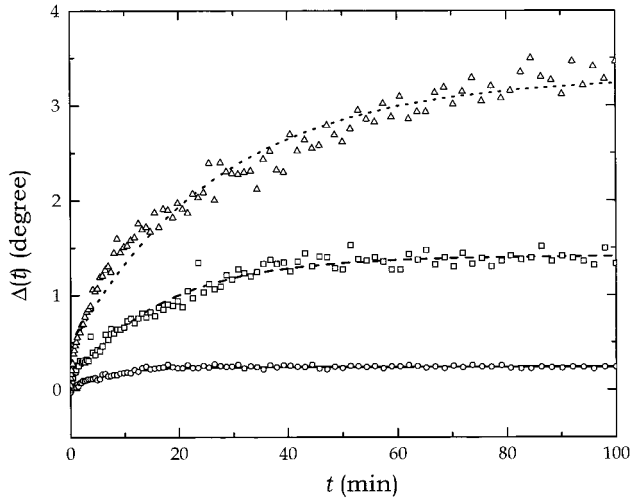


Figure 3. Time-resolved ellipsometric curves $\Delta(t)$ for adsorbed monolayers of Pluronic I obtained at $T = 20 \pm 1$ °C at different bulk concentrations in the brush regime: (\square) 7×10^{-6} mM; (\circ) 5×10^{-5} mM; (\triangle) 10^{-4} mM. The lines represent the fits of the experimental data to an exponential dependence (see the text for details).

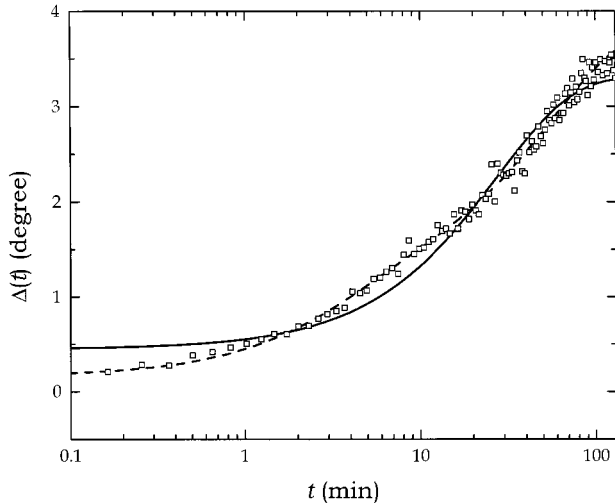


Figure 4. Detailed analysis of the TRE curve for Pluronic I at the highest studied concentration in the brush regime, $c = 10^{-4}$ mM. The lines are fits of the experimental data to a (—) monoexponential and (---) biexponential distribution (see the text for details).

weakly as the bulk concentration increases. This result is in contrast with the slight decrease in τ_{eff} with c observed in Figure 2 in the brush regime. To explain this apparent inconsistency, the τ_{eff} values obtained from the TRE experiments have been compared with those obtained from the DST measurements. Systematically lower values are obtained from the adsorption data in the TRE experiments, which are more sensitive to the mass transport, from the bulk to the interface. The DST experiments are more sensitive to the internal reorganization in the brush taking place after the mass transport is completed. This is consistent with the appearance of adsorption barriers that slow the mass transport as c (or Γ) increases, while the slower final internal reorganization stage appears to be faster with increasing Γ .

The existence of two time scales for brush formation can also be seen in TRE experiments at sufficiently large concentrations. A logarithmic representation of $\Delta(t)$ is shown in Figure 4 for $c = 10^{-4}$ mM, where one can observe the inadequacy of a monoexponential dependence. A

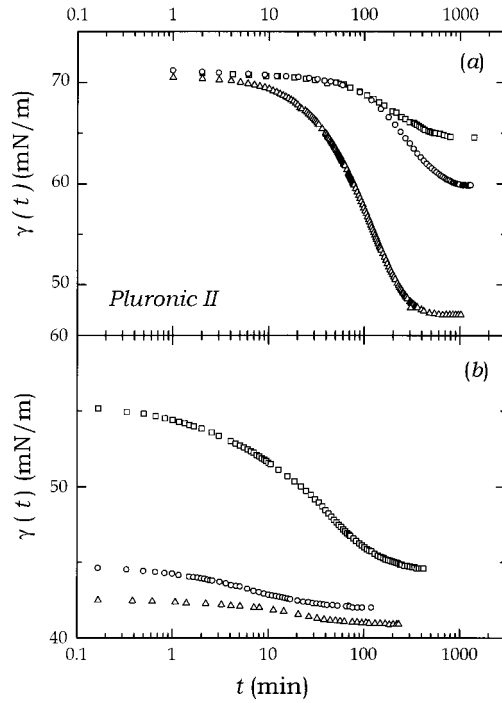


Figure 5. Experimental $\gamma(t)$ curves from DST experiments, obtained at $T = 20 \pm 1$ °C for adsorbed monolayers of Pluronic II. Bulk concentration c expressed in mM: (a) (\square) 1.24×10^{-5} ; (\circ) 1.78×10^{-5} ; (\triangle) 9.32×10^{-5} ; (b) (\square) 1.14×10^{-4} ; (\circ) 2.88×10^{-4} ; (\triangle) 9.71×10^{-4} .

simple bimodal exponential distribution more accurately fits the data, with two characteristic times, $\tau_1 \approx 200$ s, with relative amplitude 74% of the total final adsorption, and $\tau_2 \approx 2700$ s, a value very similar to $\tau_{\text{eff}} \approx 2640$ s obtained from the $\gamma(t)$ curve at a similar concentration, $c = 1.6 \times 10^{-4}$ mM. This bimodal behavior has also been observed in the DST data obtained in the coexistence region $c_1 \leq c \leq c_2$. (see the discussion in Section 5.d).

Similar DST experiments were also performed on the adsorbed monolayers of the more hydrophobic Pluronic II. Some of the experimental $\gamma(t)$ curves are shown in Figure 5. The behavior observed is similar to that exhibited by Pluronic I. Figure 6 shows that at $c > c_1 \approx 3 \times 10^{-5}$ mM. A strong decrease of the effective adsorption time τ_{eff} is observed as in Pluronic I. This value of c coincides with the beginning of the first Π plateau at $\Pi_1 \approx 25$ mN/m). Further increases in concentration above c_2 , where a complete brush is formed, causes the leveling-off of τ_{eff} in a way similar to that of Pluronic I. In this concentration regime, the $\gamma(t)$ curves extrapolate well to the solvent value γ_0 at $t \rightarrow 0$. However, and as in the case of Pluronic I, at $c \geq c_2 \approx 10^{-4}$ mM the first step of the adsorption kinetics (diffusive stage) becomes faster than 1 s, and the apparent initial value of $\gamma(t)$ is lower than γ_0 .

5. Discussion

To compare the diffusion coefficients obtained from the earlier stages of the adsorption kinetics, dynamic quasi-elastic light-scattering measurements (DQELS) of the dilute solutions were carried out to determine the diffusion coefficient D independently.¹⁵ Figure 7 shows the individual diffusion coefficient for aqueous solutions of Pluronic I as a function of polymer concentration. A lower limit, $D_0 = (0.92 \pm 0.02) \times 10^{-6}$ cm²/s, is reached at $c \approx$

(15) García, M. G.; Monroy, F.; Ortega, F.; Rubio, R. G. Unpublished results.

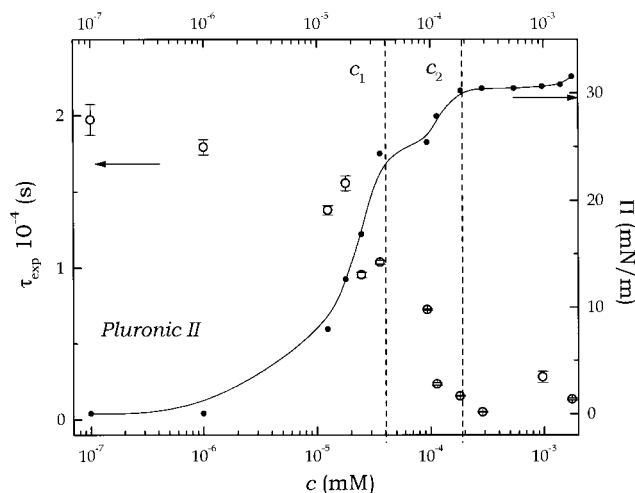


Figure 6. Effective time for surface formation τ_{eff} as a function of bulk concentration for adsorbed monolayers of Pluronic II at $T = 20 \pm 1$ °C. For comparison with the different surface regimes, the equilibrium Π - c isotherm is also shown: $c \leq c_1$, full adsorption regime; $c \geq c_2$, brush regime; $c_1 < c < c_2$, coexistence region.

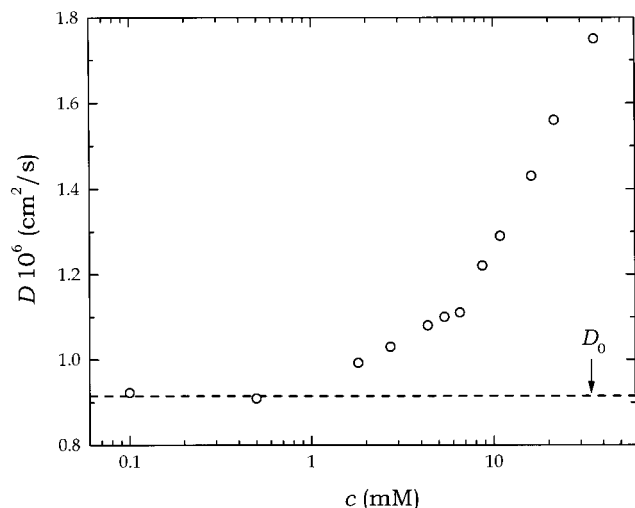


Figure 7. Individual diffusion coefficient D for Pluronic I in aqueous solution as a function of the bulk concentration (obtained from DQELS measurements). The dashed line represents the high dilution asymptotic limit.

1 mM. This high dilution value will be used in the $\gamma(t)$ and $\Gamma(t)$ analyses of the DST and TRE data.

5.a. Time-Resolved Ellipsometry. To obtain the amount of adsorbed polymer $\Gamma(t)$ from the TRE data, an analysis of $\Delta(t)$ based on eq 17 has been performed. Figure 8 shows several time-resolved adsorption curves for Pluronic I in the full adsorption and brush regimes. The short-time asymptotic behavior is clearly diffusion-controlled: $\Gamma(t) \approx 2c(D_{\text{short}}t/\pi)^{1/2}$. From the linear slopes at $t \rightarrow 0$ one obtains the diffusion coefficient shown in the inset in Figure 8 together with the value obtained from the light-scattering experiments (see Figure 7). A clear disagreement ($D_{\text{short}} \gg D_0$) between the two sets of data is found at $c \approx c_2 > 10^{-5}$ mM, the concentration at the second plateau Π_2 (see Figure 2), where a complete polymer brush is expected. This deviation confirms the appearance of more complex adsorption processes in the brush regime.

5.b. Dynamic Surface Tension. Figure 9 shows the $\gamma(t)$ data for this polymer in the full adsorption regime ($c < c_1$). Section a of this figure collects the $\Gamma - t^{1/2}$ short-time data, showing a clear linear behavior at $t \rightarrow 0$ consistent

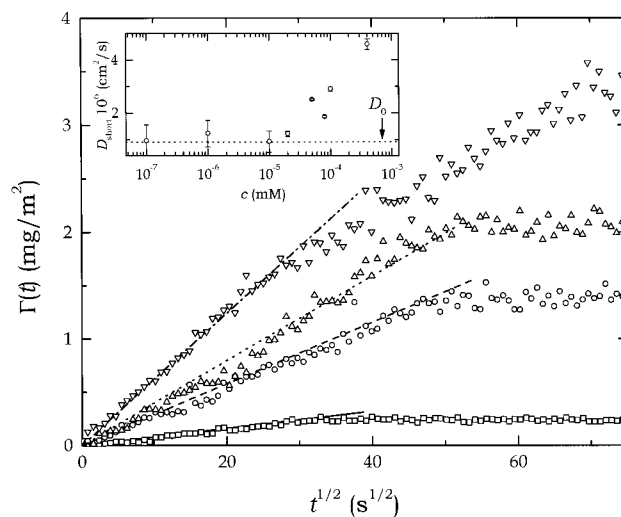


Figure 8. Short-time $t^{1/2}$ representation of the dynamic adsorption data $\Gamma(t)$ of adsorbed monolayers of Pluronic I obtained by analysis with eq 17 of the TRE results. Different bulk concentrations are shown: (\square) 2×10^{-5} mM; (\circ) 5×10^{-5} mM; (\triangle) 8×10^{-5} mM; (∇) 1×10^{-4} mM. The lines give evidence for the linear $\Gamma(t^{1/2})$ dependence at short times, indicating diffusion-like behavior in the $t \rightarrow 0$ limit. The diffusion coefficient D_{short} obtained from these fits (points) and the high dilution bulk value D_0 (dashed line), obtained from DQELS measurements, are represented in the inset.

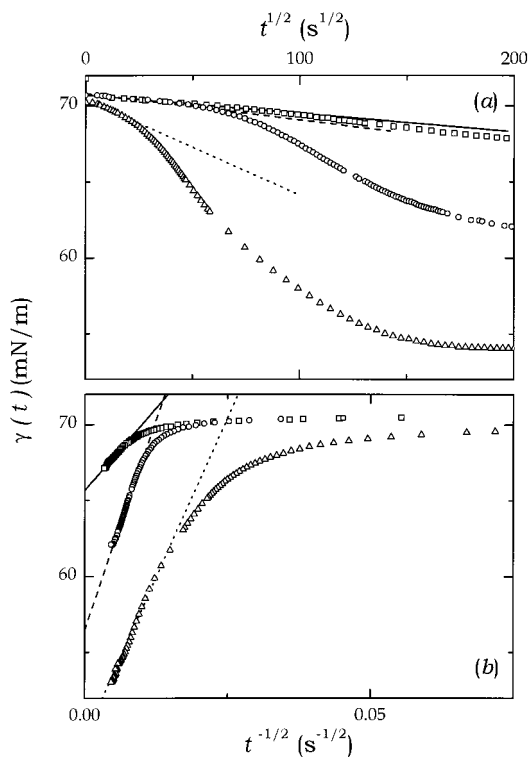


Figure 9. (a) Short-time analysis of the DST data of monolayers of Pluronic I in the full adsorption regime at different bulk concentrations: (\square) 1.7×10^{-6} mM; (\circ) 2.39×10^{-6} mM; (\triangle) 7.17×10^{-6} mM. (b) Long-time analysis of the same data in (a).

with diffusion-controlled adsorption. Strong deviations from linearity are observed at higher t ; the range of validity of the linear limit shifts to lower times as the polymer concentration increases. From the slopes of the linear $\gamma(t) - t^{1/2}$ curves at $t \rightarrow 0$, one obtains directly the diffusion coefficient D_{long} by using the asymptotic solution to the diffusion problem (see eq 5). Figure 10a shows that the calculated values in this concentration regime are in good

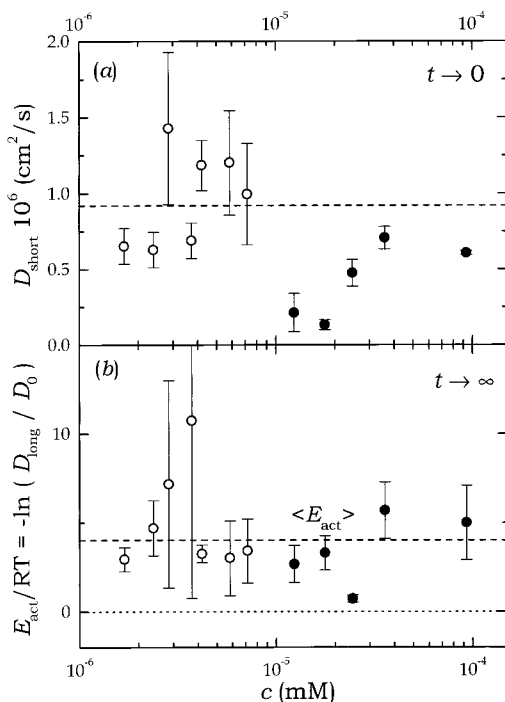


Figure 10. (a) Diffusion coefficients obtained from the short-time analysis (eq 5) of the DST data in the full adsorption regime of the monolayers of (○) Pluronic I and (●) Pluronic II at $T = 20 \pm 1$ °C. The dashed line is the value for Pluronic I obtained from DQELS measurements ($D_0 = 0.92 \times 10^{-6}$ cm²/s). (b) Estimated amount of the adsorption barrier E_{act} , obtained from the long-time analysis in the full adsorption regime. The near-universal value $E_{\text{act}} \approx 3RT$ found in other surfactants is represented by the dashed line (see details in the text).

agreement with the high dilution bulk value $D_0 = 0.92 \times 10^{-6}$ cm²/s, obtained from light-scattering measurements. As is shown in Figure 10a, slightly lower values have been obtained from the short-time representations for Pluronic II, which correlates well with the more hydrophobic character of this PPO-rich copolymer. The long-time representation in Figure 9b also points out a linear asymptotic behavior of the $\gamma(t) - t^{-1/2}$ data in the limit $t \rightarrow \infty$ for Pluronic I as predicted in eq 6. Similar behavior is found for Pluronic II.

From the limiting slopes at $t^{-1/2} \rightarrow 0$ it is possible to obtain the values of an effective coefficient diffusion $D_{\text{eff}} (=D_{\text{long}})$ which accounts for long-time kinetics deviations from the pure diffusive transport. By using previously reported equilibrium data of $\Gamma(c)$,¹ The experimental values of D_{eff} have been calculated from this long-time approach. We have found that $D_{\text{long}} < D_{\text{short}}$ in both polymers, which points out a certain deviation from the pure diffusive model at long times.

5.c. Adsorption Barrier in the Full Adsorption Regime. A method of quantitatively discussing the deviations of the calculated values of D with respect to the bulk value is to quantify the activation energy of the adsorption-desorption process (see eq 10). As bulk value D in eq 10, we have used the high dilution value, from light-scattering measurements, for Pluronic I, $D = D_0 = 0.92 \times 10^{-6}$ cm²/s, and the averaged value from the short-time data, $D = \langle D_{\text{short}} \rangle = (0.43 \pm 0.07) \times 10^{-6}$ cm²/s, for Pluronic II. The results are shown in Figure 10b; as can be observed, positive values for $E_{\text{act}} = E_A - E_D$ are obtained for both polymers at the air-water interface in the high dilution regime at $c \leq c_1$.

This activation energy, similar for both polymers, $E_{\text{act}} \approx 10$ kJ/mol $\approx 4RT$, seems to be independent of concen-

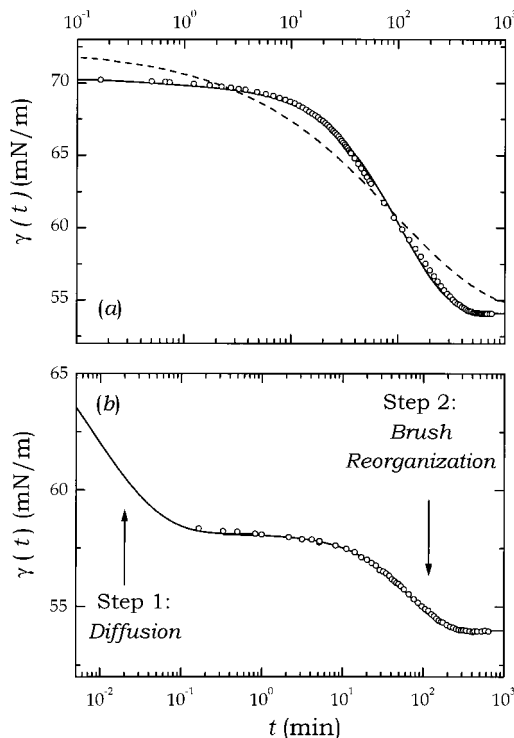


Figure 11. (a) Mixed diffusion plus sorption effects in the adsorption kinetics of Pluronic I at $c \approx c_1$ at the air-water interface: (○) experimental $\gamma(t)$ curve at 20 °C; (- -) fit to an exponential dependence; (—) to the mixed diffusion plus reorientation model in eq 11. (b) Two-step kinetics in the brush regime at $c = 6.71 \times 10^{-5}$ mM.

tration within the experimental error, at least in the high dilution regime considered here. This result is similar to earlier ones for adsorbed monolayers of a monomeric cationic surfactant¹⁶ and small polyglycol ethers and glucamides,¹⁷ where adsorption barriers also exist. The values of $E_{\text{act}} \approx 10$ kJ/mol do not depend on molecular weight, surfactant type or structure, CMC values, or the presence of micelles in the solution.¹⁷ Were reorientational mechanisms responsible for this adsorption barrier in the full adsorption regime, it should depend on molecular structure. Some authors have invoked a surface pressure driven mechanism for the adsorption barrier, accounted for by a sticking probability factor, S , proportional to the unoccupied fraction, $1 - \Theta$. As a consequence, the ability of adsorption of a polymer chain would become progressively lower at higher surface concentration. This process is obviously longer than the diffusion process; otherwise, it would not be visible in the experiments.

5.d. Bimodal Kinetics: Diffusion Plus Reorientation Mixed Mechanism. Fits of the experimental $\gamma(t)$ curves in the whole time range (from 1 s to equilibrium) have also been attempted. Figure 11a shows a typical example of diffusion-like kinetics delayed by the adsorption barrier in the concentrated (full adsorption) regime ($c \approx c_1$). A single exponential variation for diffusion-controlled adsorption is clearly inadequate. The mixed diffusion plus reorientation mechanism in eq 11 is able to describe the adsorption kinetics in this concentration regime. Both diffusion τ_D and adsorption τ relaxation times can be simultaneously calculated. The characteristic times τ are in good agreement with the effective times τ_{eff} obtained from the simpler monoexponential model.

(16) Eastoe, J.; Dalton, J. S.; Rogueda, P. G. A.; Sharpe, D.; Dong, J. *Langmuir* **1996**, *12*, 2706.

(17) Eastoe, J.; Dalton, J. S.; Rogueda, P. G. A.; Crooks, E. R.; Pitt, A. R.; Simister, E. A. *J. Colloid Interface Sci.* **1997**, *188*, 423.

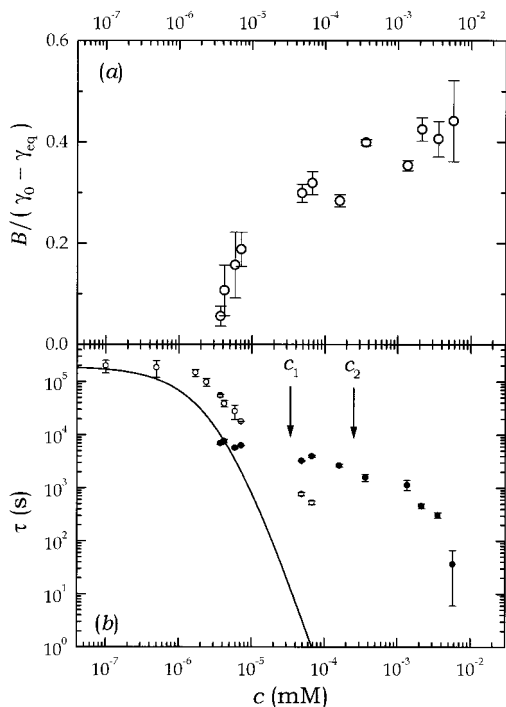


Figure 12. Dynamic properties of the adsorption kinetics of Pluronic I at the air–water interface at 20 °C, obtained from the fits of the DST experimental data in Figure 1 to eq 11: (a) relative amount of the exponential-like kinetic process in the total adsorption kinetics; (b) characteristic times for the (○) diffusion τ_D and (●) reorganization τ_R processes. The continuous line is the theoretical value for τ_D (eq 12 and 18) obtained from the parameters (a, Γ_∞) of the fits of the equilibrium γ -isotherm to the Langmuir equation of state in eq 16.

Figure 11b shows a similar analysis in the concentrated brush regime. The first diffusive step is now much faster than the final stage, and both appear clearly separated. A faster diffusive step (see eq 13) $D = D_0$ with $\tau_D \approx 0.5$ s, has been tentatively proposed in this figure as extrapolation of the experimental data at $t \rightarrow 0$ (also see the data in Figure 12). In effect, an intermediate plateau, which corresponds to the *apparent* initial stage observed in the experimental $\gamma(t > 5$ s) curves, is now predicted between the initial diffusion stage and a slower exponential-like mechanism, accounting for internal reorganization of the brush.

To summarize, we have fitted the experimental $\gamma(t)$ curves to eq 11 in the whole concentration range, obtaining the characteristic times for both diffusive-like and reorientational first-order kinetic steps, and the relative amplitude for this last reorientational stage $B/(\gamma_0 - \gamma_{eq})$. For the sake of brevity only the results for Pluronic I are displayed in Figure 12. Similar qualitative behavior has been found with the other polymer. In the dilute regime ($c < c_1$) the experimental $\gamma(t)$ curves are well described by pure diffusion ($B \rightarrow 0$); however, at higher concentrations B becomes comparable to $\gamma_0 - \gamma_{eq}$. If the mechanism for surface formation were only controlled by diffusion plus adsorption/desorption barriers, eq 13 would always be able to fit the experimental results at long times and the effective diffusion time would account for the adsorption barrier. However, good fits require the use of eq 11 above c_1 , which incorporates a supplementary kinetic process, possibly transport through the polymer brush.

Figure 12b collects the values obtained for both characteristic times, τ_D for diffusion and τ_R for the slower kinetic process. The diffusion time τ_D goes to zero at the concentration c_2 . For the sake of comparison, a theoretical

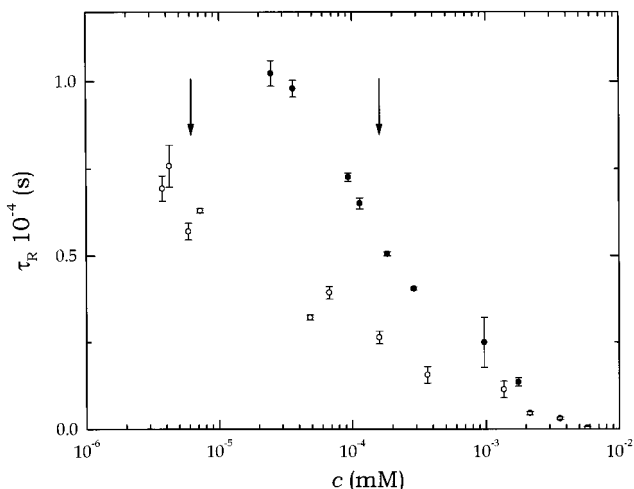


Figure 13. Characteristic time for the reorganization exponential-like process of the adsorption kinetics for both polymers: (○) Pluronic I; (●) Pluronic II. The arrows mark c_2 or bulk concentration at complete brush formation (left for Pluronic I and right for Pluronic II).

calculation of τ_D (see eq 12) based on the fits of the equilibrium surface tension γ_{eq} to the Langmuir adsorption equation (see eqs 14 and 16) has been performed at $c < c_1$:

$$\frac{d\Gamma}{dc} = \frac{\Gamma_\infty}{a} \left(1 - \frac{\Gamma}{\Gamma_\infty}\right)^2 \Rightarrow \tau_D = \frac{1}{D} \frac{\Gamma_\infty^2}{a^2} \left(1 - \frac{\Gamma}{\Gamma_\infty}\right)^4 \quad (18)$$

The theoretical values of τ_D calculated from the equilibrium quantity $d\Gamma/dc$ are also shown in Figure 12b. A good agreement is observed with the τ_D values obtained from the fits of the $\gamma(t)$ curves at concentrations $c \ll c_1$. However, at higher concentration in the full adsorption regime, $c \leq c_1$, the values of τ_D obtained from $\gamma(t)$ become higher than the theoretical prediction. This is a signature of the building up of an adsorption barrier, as already deduced from the ellipsometric $\delta\Delta(t)$ data in Figure 8. A switch to a $\gamma(t \rightarrow 0) > \gamma_0$ followed by exponential-like behavior occurs at $c \approx c_2$. The bimodal kinetics previously discussed emerges now, *i.e.*, a first diffusive step affected by an adsorption barrier (too fast to be measured by the present technique), followed by a slower kinetic stage, which is the rate limiting step of the surface formation process.

For comparison purposes, the reorientational time τ_R for the films of both polymers in the brush regime $c \geq c_2$ is shown in Figure 13. Higher τ_R values are systematically found for Pluronic II, which correlates well with the conformational image proposed for the brush phase in the previous paper.¹ A folded structure was proposed for the triblock copolymer chains with the central PPO block in the air. Pluronic I has a more open structure, as suggested from the ellipsometric data (see section 5.c in ref 1), whereas the PPO-rich Pluronic II has a near-vertical conformation. A slower kinetics is expected for brush formation for Pluronic II since the size of the central PPO block is larger, and the final highly folded equilibrium structure requires the internal reorganization of a larger number of individual bonds in the chain, as is experimentally observed.

5.e. Bimodal Kinetics and Phase Behavior. Finally, two central questions arise from the $\gamma(t)$ kinetic behavior: Which is the mechanism that makes the system switch from an adsorption barrier delayed diffusive behavior to a bimodal kinetics at $c = c_2$, where the slower reorientational mode separates clearly from the first diffusive-

like stage? why is this crossover observed in the $\gamma(t)$ data and not in the instantaneous adsorbed amount $\Gamma(t)$ obtained from the TRE data?

The explanation for these apparent discrepancies is linked to the phase transition behavior already manifested in the equilibrium properties. Indeed, when the polymers adsorb at the air–water interface, a first diffusion stage is always necessary to take the polymer chains from the bulk to the surface region. If polymer concentration in the subsurface c_s is not high enough, grafting is not possible after diffusive transport. Hence, the full adsorption is delayed by a universal entropic barrier at $c \leq c_1$. At this point, adsorption is fully attained, and the equilibrium steady state is established, $d\Gamma/dt = 0$. However, at $c > c_2$ a polymer brush is formed after the polymer chains are previously transported by diffusion from the bulk. At a certain point grafting starts, but only when the polymer concentration in the subsurface, c_s , is high enough to saturate the monolayer is there a coexistence between fully adsorbed material and brushed chains. The surface tension remains constant as long as there is phase coexistence between both phases, *i.e.*, $d\gamma/dt = (d\gamma/d\Gamma) = (d\Gamma/dt) = 0$. However, surface transport remains active, $d\Gamma/dt \neq 0$, sustaining the internal reorganization mechanisms until final steady-state equilibrium is attained. Finally, when the concentrated brush is fully formed, the additional decrease in surface tension, due to the internal reorganization of the brush is now observed (exponential relaxation).

5.f. Comparison with Kinetic Theory for Polymer Brushes. Barentin et al.¹⁸ have recently indicated that three different dynamic processes within a polymer brush might exist: *adsorption* of one chain to the brush, *desorption* with total expulsion to the bulk phase, and *density relaxation* within the brush. A conclusion of their scaling analysis for polymer brushes is that the relaxation times corresponding to the adsorption and desorption of a grafting element at the interface should be very similar. However, the total expulsion time of the grafted chain from the brush is instantaneous compared to the desorption of the grafting element. From scaling arguments the characteristic time of the adsorption–desorption process has been found to depend exponentially on the reduced energy for brush formation $E = \epsilon/k_B T$.^{18,19}

$$T_{AD} = \tau_{\text{blob}} \sigma^{-3/2} \exp E \quad (19)$$

where σ is the grafting density of the brush and τ_{blob} is a microscopic time, characteristic of the internal molecular motion in a blob subunit of the polymer chains.

Since $\tau_{\text{blob}} \approx 10^{-10}$ s, Barentin et al.¹⁸ have found that $T_{AD} \approx 10^{-2}$ s for most of the polymer brushes. This theoretical prediction is in qualitative agreement with the time scale at which the adsorption–desorption initial stage might appear in our experimental $\gamma(t)$ curves obtained in the brush regime (see Figures 11b and 12b).

On the other hand, a slower motion corresponding to density relaxation within the brush might occur at higher times, when the brush has already been adsorbed from the bulk. In this first-order kinetic process, $d\sigma(t)/dt \approx -(1/T_R)\sigma(t)$, is characterized by a relaxation time T_R ($\gg T_{AD}$) given by

$$T_R = \tau_{\text{blob}} \sigma^{-3/2} \exp(2E - N\sigma) \quad (20)$$

where N is the polymerization degree of the polymer chains.

Equation 20 shows that large values of E strongly increase the relaxation time; thus, a dense brush expels polymers more easily. This is the trend observed in Figure 12b for brushes of Pluronic I; the experimental values of the internal relaxation time τ_R ($\sim T_R$) slightly decrease as polymer concentration increases. The two relaxation times, adsorption (eq 19) and internal relaxation (eq 20), are simply related through two constituent parameters, brushing energy E and grafting density σ , *i.e.*, $T_R = T_{AD} e^{(E-N\sigma)}$.

Barentin et al.¹⁸ conclude that the energetic cost to dissolve one hydrophobic end in water is in the range 10–15 for most brushes. Since the free energy of the brush state is greater than a fully adsorbed monolayer, E might be considered to be similar to or greater than the adsorption barrier pointed out in the full adsorption regime, $E \geq E_{\text{act}}/RT \approx 4$ (see section 5.c). Moreover, in the limit $N\sigma \rightarrow 1$ (concentrated brush) the expression given in eq 20 does not depend on the grafting density, $T_R \approx \tau_{\text{blob}} N^{3/2} e^{(2E-1)}$. Then, if one considers $E \approx 10$ and $N = 180$, which is the case for Pluronic I, one obtains $T_R \approx 10^2$ – 10^3 s. This estimation agrees well with the experimental values of the relaxation time of the slower process experimentally observed for both polymers in the brush regime (see Figures 2, 6, and 12b), thus confirming the *reorientational* character of the final stage of the observed kinetics.

6. Conclusions

For small polymer concentrations, a regime of full adsorption is observed where a diffusion-mediated adsorption kinetics has been evidenced. The diffusion coefficients obtained from the purely diffusive initial stages are in excellent agreement with the values independently measured by DQELS for Pluronic I. As for small surfactants, the presence of a near-universal adsorption barrier limits the final adsorption.

For larger polymer concentrations, a brush is formed at the surface and an additional slower kinetic process appears. Slow molecular rearrangements in the concentrated brush could be at the origin of this rate-limiting stage. The relaxation times for this slower motion, obtained by fitting the experimental DST curves to a first-order kinetic equation, are in quantitative agreement with the predictions of the scaling theory for the relaxation of the internal density of a polymer brush.

The first-order character of the full adsorption \rightarrow brush phase transition, evidenced from the equilibrium behavior, is also observed in the adsorption kinetics. Intermediate phase-coexistence plateaus appear in the $\gamma(t)$, which manifest coexistence between fully and partially adsorbed material before the final equilibration of the brush is completed.

Acknowledgment. This work was supported in part by the Fundación Ramón Areces and by DGES under grant PB96-609. F. M acknowledges the Centre d'Etudes de Physique Théorique et Nucléaire (CEPHYTEN, France) for financial support under Contract 98/44-Institut Français du Pétrole.

(18) Barentin, C.; Muller, P.; Joanny, J. F. *Macromolecules* **1998**, *31*, 2198.

(19) Witmer, J.; Johner, A.; Joanny, J. F. *J. Chem. Phys.* **1994**, *101*, 4379.